

Extratropical cyclones act as a 'bridge' to the concurrent impact of ENSO on the Arctic oscillation during boreal winter

Article

Published Version

Creative Commons: Attribution 4.0 (CC-BY)

Open Access

Qian, S., Hu, H., Hodges, K. I. ORCID: https://orcid.org/0000-0003-0894-229X, Zhu, Y., Yang, X.-Q. and Wang, Y. (2025) Extratropical cyclones act as a 'bridge' to the concurrent impact of ENSO on the Arctic oscillation during boreal winter. Geophysical Research Letters, 52 (20). e2025GL116719. ISSN 0094-8276 doi: 10.1029/2025GL116719 Available at https://centaur.reading.ac.uk/123683/

It is advisable to refer to the publisher's version if you intend to cite from the work. See <u>Guidance on citing</u>.

To link to this article DOI: http://dx.doi.org/10.1029/2025GL116719

Publisher: American Geophysical Union

All outputs in CentAUR are protected by Intellectual Property Rights law, including copyright law. Copyright and IPR is retained by the creators or other copyright holders. Terms and conditions for use of this material are defined in the End User Agreement.

www.reading.ac.uk/centaur



CentAUR

Central Archive at the University of Reading Reading's research outputs online



Geophysical Research Letters



RESEARCH LETTER

10.1029/2025GL116719

Key Points:

- Single, double, and opposite El Niño-Southern Oscillation events exert significant and comparable concurrent impacts on the Arctic Oscillation
- The translation of extratropical cyclones (ECs) over the North Atlantic to the Arctic is key process in this concurrent impact
- The horizontal heat advection from the Pacific to the Atlantic decides the genesis location and poleward translation of the ECs

Supporting Information:

Supporting Information may be found in the online version of this article.

Correspondence to:

H. Hu, huhaibo@nju.edu.cn

Citation:

Qian, S., Hu, H., Hodges, K. I., Zhu, Y., Yang, X.-Q., & Wang, Y. (2025). Extratropical cyclones act as a "bridge" to the concurrent impact of ENSO on the Arctic Oscillation during boreal winter. *Geophysical Research Letters*, 52, e2025GL116719. https://doi.org/10.1029/2025GL116719

Received 25 APR 2025 Accepted 8 OCT 2025

Author Contributions:

Conceptualization: Haibo Hu Funding acquisition: Haibo Hu Investigation: Shengyi Qian Methodology: Haibo Hu, Kevin I. Hodges Supervision: Haibo Hu Visualization: Shengyi Qian Writing – original draft: Shengyi Qian, Haibo Hu

Mriting – review & editing: Shengyi Qian, Haibo Hu, Kevin I. Hodges, Yimin Zhu, Xiu-Qun Yang, Yuanheng Wang

© 2025. The Author(s).

This is an open access article under the terms of the Creative Commons

Attribution License, which permits use, distribution and reproduction in any medium, provided the original work is properly cited.

Extratropical Cyclones Act as a "Bridge" to the Concurrent Impact of ENSO on the Arctic Oscillation During Boreal Winter

Shengyi Qian¹, Haibo Hu¹, Kevin I. Hodges², Yimin Zhu³, Xiu-Qun Yang¹, and Yuanheng Wang⁴

¹CMA Key Laboratory for Climate Prediction Studies, School of Atmospheric Sciences, Nanjing University, Nanjing, China, ²Department of Meteorology and National Centre for Atmospheric Science, University of Reading, Reading, UK, ³College of Meteorology and Oceanography, National University of Defense Technology, Changsha, China, ⁴China Yangtze Power Co., Ltd., Yichang, China

Abstract This study investigates that the concurrent influence of El Niño-Southern Oscillation (ENSO) on the Arctic Oscillation (AO) mediated through the poleward translation of extra-tropical cyclones (ECs) over the North Atlantic is more significant than the one-year-lagged impact of ENSO through poleward propagating atmospheric angular momentum. Specific results show that during El Niño (La Niña) winter, the anomalous atmospheric horizontal heat advection from the Pacific to the Atlantic, which is caused by the southward (northward) displacement of the westerly jet stream, enhances (weakens) the atmospheric baroclinicity over the subtropical North Atlantic. Subsequently, the changed baroclinicity drives intensified (reduced) baroclinic energy conversion from the eddy available potential energy to the eddy kinetic energy, which shifts the genesis locations of ECs southward (northward) and suppresses (enhances) their poleward translation into the Arctic. Ultimately, through the combined thermodynamic and dynamical forcing associated with EC activity, the negative (positive) AO pattern is generated in the concurrent winter.

Plain Language Summary El Niño-Southern Oscillation (ENSO) exerts both concurrent and one-year-lagged impacts on the Arctic Oscillation (AO). This study demonstrates that the concurrent influence of ENSO by modulating the poleward translation of extra-tropical cyclones (ECs) over the North Atlantic is stronger than the one-year-lagged influence of ENSO by inducing poleward propagating atmospheric angular momentum. Specific results show that the anomalous tropical Pacific sea surface temperature in El Niño (La Niña) winter leads to the southward (northward) displacement of the westerly jet stream and its accompanying atmospheric horizontal heat advection from the Pacific to the Atlantic. The southward (northward) shifted horizontal heat advection enhances (weakens) the atmospheric baroclinicity over the subtropical North Atlantic. Subsequently, the changed baroclinicity drives intensified (reduced) baroclinic energy conversion from the eddy available potential energy to the eddy kinetic energy, whereas the conversion of barotropic energy is negligible. The enhanced (weakened) baroclinicity shifts the genesis locations of ECs southward (northward) and suppresses (enhances) their poleward translation into the Arctic. Ultimately, through the combined thermodynamic and dynamical forcing associated with EC activity, the Arctic shows negative (positive) AO pattern at the same El Niño (La Niña) winter. This study is conducive to the understanding of tropics-Arctic interaction.

1. Introduction

The El Niño-Southern Oscillation (ENSO), a coupled ocean-atmosphere phenomenon in the tropics, manifests as anomalous sea surface temperature (SST) variability in the equatorial central-eastern Pacific (Bjerknes, 1969). Extensive studies have shown that ENSO modulates the global weather and climate (McPhaden et al., 2006). ENSO can regulate extratropical temperature and precipitation anomalies in the Northern Hemisphere (NH) through teleconnection mechanisms (Trenberth et al., 1998), with documented links to extreme weather events (Arblaster & Alexander, 2012; Dai et al., 1997; Lu et al., 2025). Recent studies have highlighted that ENSO variability is influenced by anthropogenic global warming (Cai et al., 2018, 2021, 2023; Chen et al., 2024; Yeh et al., 2018). The canonical ENSO lifecycle exhibits a phase-locking feature. ENSO typically initiates during the boreal spring or summer, reaches its peak in winter, and gradually decays in the following spring (Neelin et al., 2000; Rasmusson & Carpenter, 1982). ENSO events show significant internal complexity (Timmermann et al., 2018) and diversity (Capotondi et al., 2015). Based on the diverse spatial distribution of SST anomalies,

OIAN ET AL. 1 of 12

ENSO events can be categorized into Eastern Pacific and Central Pacific types (Ashok et al., 2007; Fu et al., 1986; Kao & Yu, 2009). However, a pronounced asymmetry exists between El Niño and La Niña events, with La Niña events showing weaker spatial heterogeneity compared to their warm counterparts (Kug & Ham, 2011). Further analysis reveals the diversity of the temporal evolution patterns of ENSO events (Choi et al., 2013; Scaife et al., 2024; Tokinaga et al., 2019), including those that only exist for a single year (individual events), those that persist for 2 years (double events), and those that reverse their phase in the following year (opposite events). Choi et al. (2013) found that El Niño events are more likely followed by La Niña events, whereas La Niña events show reduced probability of transitioning to El Niño events due to their high sensitivity to external forcing. Moreover, Tokinaga et al. (2019) identified divergent forcing effects on the North Atlantic SST between individual and double La Niña events.

ENSO is also able to modulate the Arctic Oscillation/North Atlantic Oscillation (AO/NAO) during the concurrent boreal winter through poleward-propagating Rossby waves (Hoskins & Karoly, 1981; Li & Lau, 2012; Quadrelli & Wallace, 2002; Toniazzo & Scaife, 2006). The AO, also termed the Northern Annular Mode, represents the leading empirical orthogonal function (EOF) mode of extratropical sea level pressure (SLP) anomalies over the NH in boreal cold season, characterized by a seesaw pattern between polar and mid-latitude regions, constituting the dominant variability mode of the climate in the NH (Thompson & Wallace, 1998). Spatially, the AO presents significant zonal symmetry and equivalent barotropic vertical structures (Wallace & Thompson, 2002). While the AO and the NAO are dynamically coupled across spatiotemporal scales (Feldstein & Franzke, 2006; Hurrell, 1995; Wallace, 2000), their relationship has remained debatable (Ambaum et al., 2001; Deser, 2000; Wallace & Thompson, 2002). Wallace (2000) hypothesized that the formation of the AO is due to eddy-mean flow interactions and that the AO fundamentally reflects the mid-latitude jet stream intensity. In addition, the AO can respond to the occurrence of an anomalous stratospheric circulation (Baldwin & Dunkerton, 1999, 2001; Baldwin et al., 1994), and this stratospheric precursor signal (anomalous stratospheric circulation) can be used as a predictor of the AO (Baldwin et al., 2003). A very recent study further demonstrated that ENSO can also impact the AO/NAO variability 1 year later in boreal winter (Scaife et al., 2024) through the poleward propagation of atmospheric angular momentum that still persists after ENSO decay (Scaife et al., 2022).

The poleward movement of extratropical cyclones (ECs), especially those in the North Atlantic region, has been shown to be closely related to the changes in the AO (Qian et al., 2025). However, some studies have also revealed that ENSO can affect the atmospheric baroclinic instability in remote areas (Machado et al., 2021) and thus regulate the generation and activity of ECs in the simultaneous winter (Eichler & Higgins, 2006; Grise et al., 2013; Plante et al., 2015; Reboita et al., 2015; H. S. Wang & Mullens, 2024), which may be associated with the response of the westerly jet stream to ENSO (Manney et al., 2021; Quadrelli & Wallace, 2002; Shapiro et al., 2001; Wang et al., 2024). Schemm et al. (2018) found that the number of ECs in the Gulf Stream region increased in warm ENSO years, and decreased in cold ENSO years, due to the synergistic effect of transient eddies and stationary waves induced by tropical signals.

Motivated by these previous studies, it is obvious that ECs can be influenced by cold and warm ENSO events. On the other hand, ECs over the North Atlantic are linked to the interannual variability of the AO through the poleward translation of ECs. So, this study aims to answer the following questions: does the interannual variability of the tropical Pacific SST affect the Arctic SLP and atmospheric circulation by modulating the activity of ECs over the North Atlantic? What is the difference in the influences on the AO between three different ENSO types (individual, double and opposite events)? What is the relative importance of the lagged effect of ENSO on the AO through poleward propagating atmospheric angular momentum in the previous winter versus the concurrent effect of ENSO in the same winter? Section 2 introduces the data and methods used in this study. Section 3 demonstrates the role of ECs and corresponding physical mechanism in the process of ENSO affecting the AO. The last Section provides the summary and discussion.

2. Data and Methods

In order to obtain a sufficient number of event samples and conduct an analysis of physical mechanisms, the reanalysis data utilized in this study is the NOAA-CIRES-DOE Twentieth Century Reanalysis project version 3 (20CRv3). The 20CR uses an ensemble filter data assimilation method which directly estimates the most likely state of the global atmosphere for each 3-hr period. These reanalyzes assimilate only surface observations of synoptic pressure into NOAA's Global Forecast System and prescribe SST and sea ice distribution to estimate the

QIAN ET AL. 2 of 12

atmospheric physical quantities of temperature, pressure, wind, moisture and so on (Slivinski et al., 2019). Previous studies have demonstrated that the 20CR data sets perform well in the detection of ECs over the NH (Wang et al., 2013, 2016), as well as in the reconstruction of historical windstorms (Hawkins et al., 2023). Compared to the older version 2c of 20CR (6-hourly and T62 from 1,000 to 10 hPa) used in Wang et al. (2013, 2016), the 20CRv3 has more members and higher spatiotemporal resolution (3-hourly and T254 from 1,000 to 1 hPa). Spectral resolutions T62 and T254 represent the triangular truncation at the wave numbers 62 and 254 respectively. Notably, 20CR typically only assimilate surface observations which can change significantly in time and space over time which can induce spurious trends (Bengtsson et al., 2004). The ensemble averaged 20CRv3 data set from 1806 to 2015 is obtained from the NOAA Physical Sciences Laboratory, with temporal resolution of 3hourly, daily, and monthly and spatial resolution of $1^{\circ} \times 1^{\circ}$, whereas the 80 members of 20CRv3 data set are downloaded from the National Energy Research Scientific Computing Center. To verify the reliability of the 20CRv3 data set, we compared ENSO and AO events (Scaife et al., 2024) identified using 20CRv3 with those identified by the HadISST and the HadSLP2 data sets from the Met Office Hadley Center (Allan & Ansell, 2006; Rayner et al., 2003). The leading EOF patterns of the SST over the tropical oceans (20° N-20° S) (Figure S1 in Supporting Information S1) and the SLP over the NH extra-tropics (20°-90°N) (Figure S2 in Supporting Information S1) in boreal winter (DJF) are in high agreement between those produced from 20CRv3 and the data sets from the Hadley Center. However, the spread between the 80 members of 20CRv3 is relatively large before 1870. Hence we select the winter (DJF) periods from 1870 to 2014 for the analysis. ENSO events are identified based on the Nino3.4 index defined as the regional averaged (5°N-5°S; 170°-120°W) tropical Pacific SST (Trenberth, 1997), the AO index is defined as the time series of the leading EOF mode of the SLP anomalies over the domain poleward of 20° N (Thompson & Wallace, 1998), and the NAO index is defined as the time series of the leading rotated EOF mode of the 500-hPa geopotential height anomalies over the NH (Barnston & Livezey, 1987). Following Scaife et al. (2024), ENSO events are defined as those in which the Nino3.4 index anomalies exceed 0.5 K and include 43 El Niño and 49 La Niña events. The data is not detrended and the anomalies are relative to the full record. This does not affect the results as the use of composites is in terms of differences between El Niño and La Niña events.

The detection of ECs is obtained using the automatic tracking algorithm TRACK (Hodges, 1994, 1995, 1996, 1999). The 850-hPa relative vorticity derived from 3-hourly wind fields is utilized to identify and track ECs as described by Hoskins and Hodges (2002, 2005). The vorticity is first spectrally filtered to remove total wavenumbers 0–5 and truncated to triangular truncation at 63 waves (T63) to remove the large-scale background circulation and small-scale noise before identification of the ECs. Vorticity maxima are then identified in the NH on a polar sterographic projection that exceed 1.0×10^{-5} s⁻¹ and linked in time based on the minimization of a cost function for track smoothness subject to adaptive constraints on displacement distance and track smoothness. Following the tracking, tracks with a lifetime shorter than 1 day and a displacement less than 500 km are removed from the track data sets. Since the ensemble mean of 20CR is not applicable for the ECs identification (Wang et al., 2013), the analysis of ECs involved in this paper is based on the ensemble mean after tracking all 80 members separately. The density of the ECs is computed by counting the number of ECs passing through a certain grid point. The ECs whose center positions are within 555 km (about 5° geodesic) of the grid point are considered to pass through that grid point. The density is weighted by cos(latitude) considering the sphericity of the Earth.

The atmospheric energy conversion of the eddy kinetic energy (EKE) can be diagnosed by the following formulas (Cai et al., 2007), namely the barotropic energy conversion (BTEC) from the mean kinetic energy (MKE) to the EKE and the baroclinic energy conversion (BCEC) from the eddy available potential energy (EAPE) to the EKE:

BTEC =
$$\frac{P_0}{g} \left[\frac{1}{2} \left(\overline{v'^2} - \overline{u'^2} \right) \left(\frac{\partial \overline{u}}{\partial x} - \frac{\partial \overline{v}}{\partial y} \right) + \left(-\overline{u'v'} \right) \left(\frac{\partial \overline{v}}{\partial x} + \frac{\partial \overline{u}}{\partial y} \right) \right]$$
(1)

$$BCEC = -C_1 \left(\overline{\omega_p' T'} \right) \tag{2}$$

where $C_1 = \left(\frac{P_0}{p}\right)^{\frac{C_v}{C_p}} \frac{R}{g}$, $P_0 = 1000$ hPa, R is the gas constant of dry air, g is the gravitational constant, C_v and C_p are the specific heat capacity of dry air at the constant pressure and volume, respectively, ω_p is the vertical velocity

OIAN ET AL. 3 of 12

(units: Pa/s). The overbar represents the winter mean and the prime denotes the deviation from the winter mean. The units of the energy conversion are W/m^2 .

The meridional temperature gradient is able to be used as an indicator of the atmospheric baroclinicity which has been demonstrated to significantly affect the occurrence and development of the ECs (Anthes et al., 1983; Hoskins & Valdes, 1990; Inatsu & Terakura, 2012; Roebber, 1984; Sanders & Gyakum, 1980; Yoshiike & Kawamura, 2009; Yu et al., 2025). The tendency diagnostic equation of the meridional temperature gradient can be obtained by taking the partial derivative of the temperature tendency diagnostic equation in the meridional direction, and its equation is as follows:

$$\frac{\partial}{\partial t} \left(\frac{\partial T}{\partial y} \right) = -\frac{\partial}{\partial y} (V \cdot \nabla T) + \frac{\partial}{\partial y} (\omega_p \sigma) + \frac{\partial}{\partial y} \left(\frac{\dot{Q}}{c_p} \right) \tag{3}$$

where $\sigma = \frac{RT}{pc_p} - \frac{\partial T}{\partial t}$ is the static stability, \dot{Q} is the diabatic heating rate. The first two terms on the right-hand side of Equation 3 represent the effects of horizontal and vertical temperature advection respectively, whereas the last term represents the effect of diabatic heating containing sensible, latent, and radiative heating. According to Yanai et al. (1973), the atmospheric apparent heat source can be expressed as:

$$\frac{\dot{Q}}{c_p} = \frac{\partial T}{\partial t} + V \cdot \nabla T - \omega_p \sigma \tag{4}$$

In addition, the wave activity flux (Takaya & Nakamura, 2001) and Eady growth rate (Lindzen & Farrell, 1980) are also used for diagnostic analysis.

3. Results

Our composite results of ENSO events (El Niño minus La Niña) are consistent with those in Scaife et al. (2024). In the concurrent winter of El Niño (La Niña) events, a negative (positive) AO pattern is induced in the Arctic region, while in the following winter, a positive (negative) AO pattern is stimulated (Figures 1a and 1e). Figures 1b–1d show that the corresponding negative AO phase is still exhibited in the concurrent winter in different ENSO types (individual, double, and opposite events). The individual, double, and opposite ENSO events comprise 16 (18), 11 (17), and 16 (14) El Niño (La Niña) events, respectively. Although the opposite ENSO events show negative SLP anomalies in the polar regions, the difference in SLP between the mid-latitudes and the polar regions remains negative.

The situations in the following winter of distinct ENSO types are completely different. In the individual ENSO events, the AO in the following winter is only affected by the poleward propagating atmospheric angular momentum induced by the ENSO event of the previous year (Figure 1f). While in the double and opposite ENSO events, the AO in the following winter is also modulated by the ENSO in the following winter. For double ENSO events, this counteracting effect weakens the amplitude of the AO in the following winter (Figure 1g). For opposite ENSO events, a stronger AO pattern is induced in the following winter due to the superimposed effect (Figure 1h). Among the three types of ENSO events, the behavior of the poleward propagating atmospheric angular momentum is highly consistent (Figure S3 in Supporting Information S1). Therefore, in the following winter of El Niño (La Niña) events, an AO positive (negative) phase pattern should occur in the Arctic region in theory. However, for double ENSO events, in the following winter there is not a weakened corresponding AO pattern but a pattern that completely transforms into a opposite AO phase forced by the ENSO events in the following winter, indicating that the concurrent influence of ENSO on the AO is more significant than the one-year-lagged influence of ENSO caused by the poleward propagating atmospheric angular momentum.

Based on the preceding analysis, we have identified that the concurrent impact of ENSO on the AO is more significant than that with a one-year-lagged influence. However, previous studies have only revealed the influence of poleward propagating Rossby waves induced by ENSO on the AO in the concurrent winter. Then, what role do the ECs play in the concurrent influence of ENSO on the AO? As shown in Figure 2, composite results of several indices are given during ENSO events. Among the total ENSO events, the significances between the difference in means between the number of ECs translating from the North Atlantic region to the Arctic for the

OIAN ET AL. 4 of 12

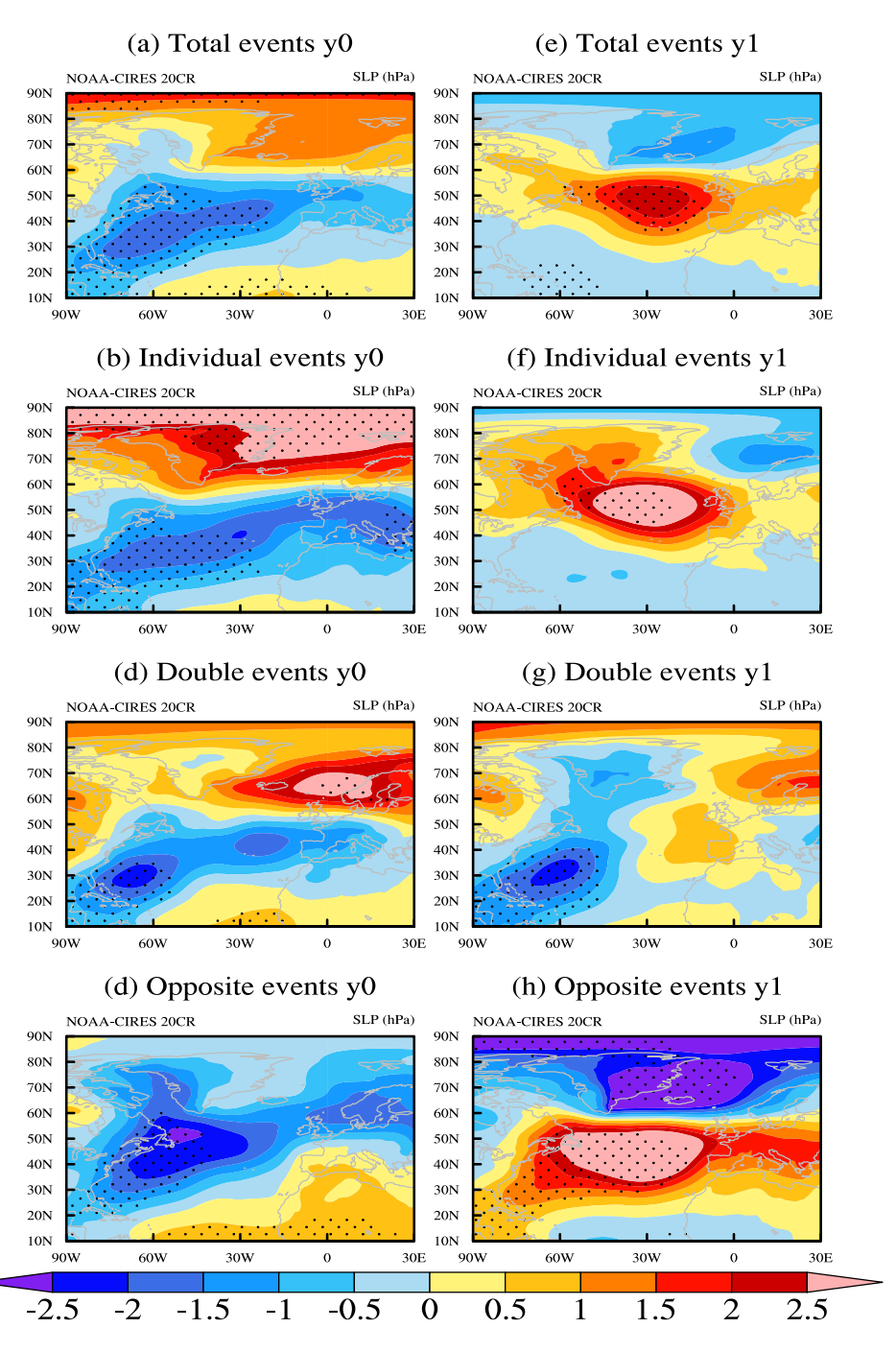


Figure 1. The sea level pressure (units: hPa) composites of El Niño-Southern Oscillation (ENSO) events (El Niño minus La Niña) in the concurrent winter and in the following winter. The composites for (a) total, (b) individual, (c) double, and (d) opposite ENSO events in the concurrent winter. (e)–(h) The same as (a)–(d), but for the results in the following winter. The black dots denote the area with significance of 95% confidence level by student-t test.

separate El Niño and La Niña winters, as well as the AO and the NAO index, pass the Student's *t*-test at 95% level in the concurrent winter, while those in the following winter do not. This is because the AO in the following winter is simultaneously affected by the ENSO in the previous winter and in the same winter, and these influences may be superimposed or counteracted for the AO. Under the classification of ENSO events, due to the small sample size, only the indices of the individual ENSO events in the concurrent winter can pass the significance test (Scaife et al., 2024). The reason the NAO index in the following winter of the opposite ENSO events can pass the

QIAN ET AL. 5 of 12

from https://agupubs.onlinelibrary.wiley.com/doi/10.1029/2025GL116719 by NICE, National Institute for Health

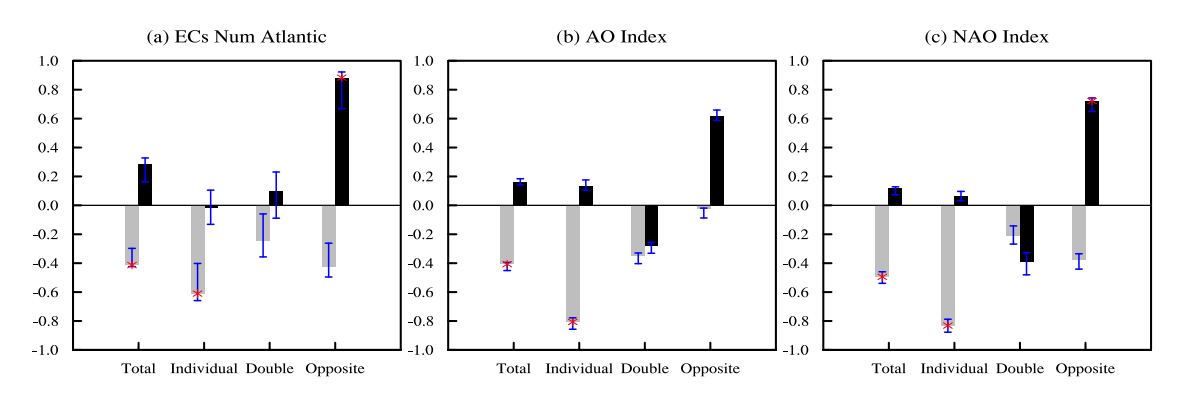


Figure 2. The composites of standardized indices in different El Niño-Southern Oscillation (ENSO) events (El Niño minus La Niña) for (a) the ensemble averaged number of the extratropical cyclones translating from the North Atlantic region into the Arctic per winter, (b) the Arctic Oscillation, and (c) the NAO. The gray and black bars represent the results in the concurrent winter and in the following winter, respectively. The top and bottom of the blue lines indicate the first quartile and third quartile in ascending order of the results of 80 members in the 20CRv3, separately. The red stars indicate the indices with significance of 95% confidence level by student-t test. The *x*-axis is the different types of ENSO events.

significance test is that the superimposed effect of the 2 years of ENSO makes the NAO have a larger amplitude. This result further supports that the concurrent influence of ENSO on the AO is more important.

The ENSO events can affect the AO in the concurrent winter by regulating the activity of the ECs over the North Atlantic because the number of the ECs translating from the mid-latitudes to the Arctic which is closely related to the AO (Qian et al., 2025). During El Niño years, the genesis positions of the ECs in the North Atlantic are shifted southward, and there are more ECs generated in the key response area (green box in Figure 3a), which is consistent with the study of Schemm et al. (2018). Further analysis finds that this may be associated with the abnormal atmospheric temperature distribution over the North Atlantic region (Figure 3b). Such a temperature anomaly distribution leads to an abnormal meridional gradient of temperature (Figure 3c), intensifying the atmospheric baroclinicity in the key response area during El Niño years. The track density, temperature, and meridional temperature gradient distributions are consistent in the composites of different ENSO types (Figure S4 in Supporting Information S1).

The MKE and EAPE are able to convert into EKE to provide the energy required for the development of the ECs. The EKE in the key response area is mainly converted from the EAPE of the BCEC during El Niño years, while the BTEC term from the MKE is very small (Figures 3d–3f). Under such circumstances, the translation of the ECs toward the Arctic from the North Atlantic decreases, thus generating the SLP anomaly pattern of the AO negative phase over the extratropics. In La Niña years, the atmospheric baroclinicity in the key response area weakens, and the BCEC from the EAPE to the EKE decreases, resulting in the genesis position of ECs over the North Atlantic being shifted to the north (Figure S5 in Supporting Information S1). Therefore, more ECs translate toward the Arctic, leading to the occurrence of the AO positive phase pattern.

The temperature anomaly over the North Atlantic during ENSO events leads to the enhancement of atmospheric baroclinicity, which in turn affects the genesis positions of the ECs over the North Atlantic and induces different SLP anomaly patterns of the AO phase. Here, we need to answer the question is this anomalous temperature distribution forced by the SST in the North Atlantic or caused by the changes in the atmosphere itself? The distribution of SST anomalies is very similar to that of the atmospheric temperature (Figure 3g), and in El Niño (La Niña) years, there are positive (negative) meridional gradient anomalies of SST in the key response area (Figure 3h). Besides, the atmospheric baroclinicity in the north of the key response area is weakened (enhanced). The changes in the atmospheric baroclinicity lead to the southward shift in the genesis location of cyclones during El Niño years. However, the net heat fluxes indicate (Figure 3i) that this anomalous SST distribution is caused by the forcing from the atmosphere above it. The meridional gradient anomalies of SST correspond to the anomalous meridional gradient of net heat flux from the atmosphere to the ocean at the sea surface. Therefore, the atmospheric temperature anomaly over the North Atlantic is not dominated by the SST in the North Atlantic.

During El Niño (La Niña) years, there is an intensification of the westerly wind anomaly south to the climatological jet axis over the North Pacific. (Figure S6 in Supporting Information S1). Such an abnormal wind field will drive abnormal atmospheric horizontal temperature advection toward the North Atlantic, so we examine each

OIAN ET AL. 6 of 12

from https://agupubs.onlinelibrary.wiley.com/doi/10.1029/2025GL116719 by NICE, National Institute for Health and Care Excellence, Wiley Online Library on [22/10/2025]. See the Terms and Conditions (https://onlinelibrary.wiley.com/rems

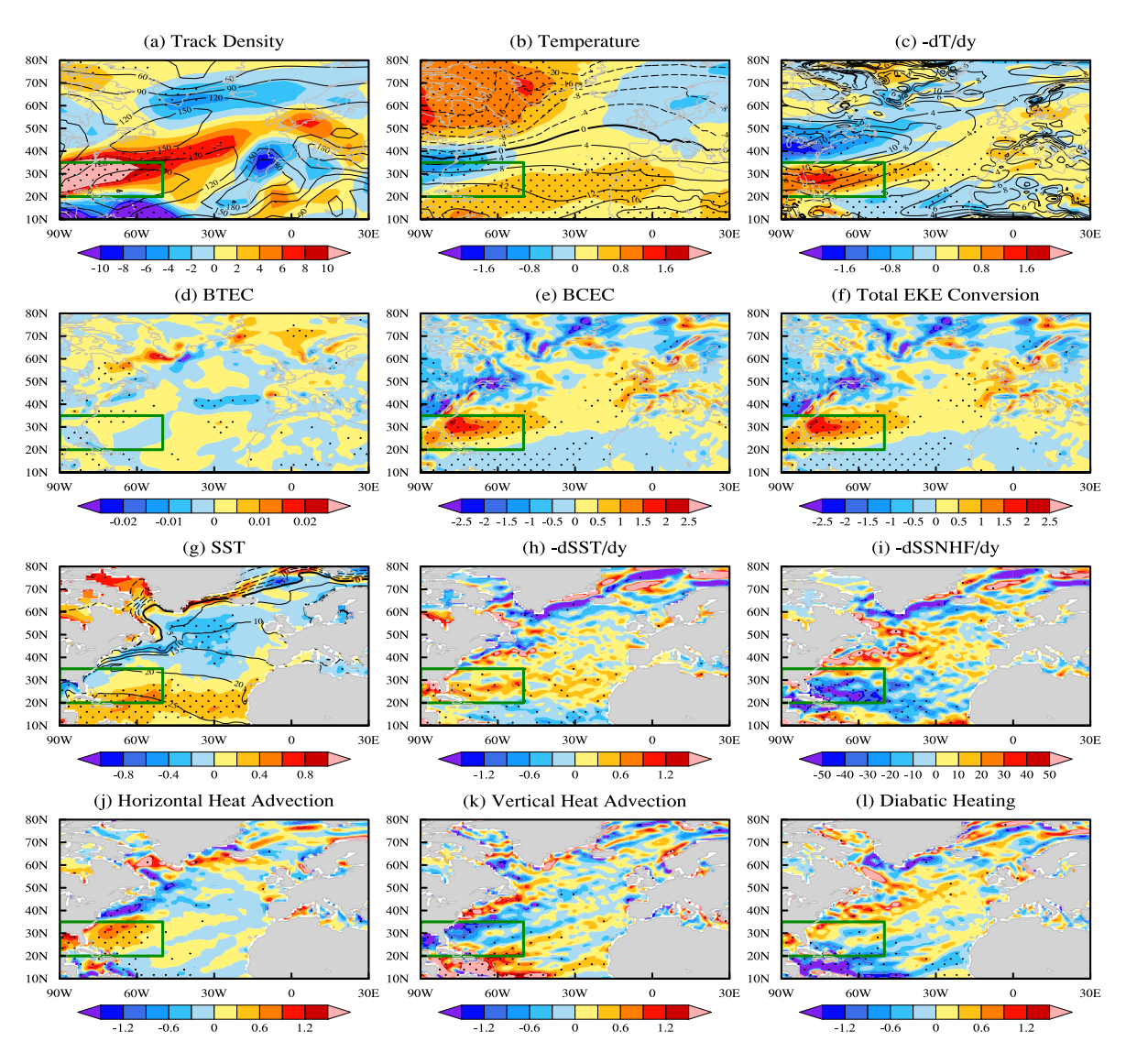


Figure 3. The composites of total El Niño-Southern Oscillation events (El Niño minus La Niña) in the concurrent winter for (a) track density (units: times/winter), (b) temperature (units: K) and (c) meridional temperature gradient (units: K/1,000 km) at 850 hPa respectively, where the contours in (a)–(c) are corresponding climatology. The same as (a)–(c), but for the composites of (d) the barotropic energy conversion (BTEC) from the MEK to the eddy kinetic energy (EKE), (e) the baroclinic energy conversion (BCEC) from the eddy available potential energy to the EKE, (f) the total EKE conversion (i.e., the sum of the BTEC and the BCEC), (g) the sea surface temperature (SST) (units: K) where the contours indicate corresponding climatology, (h) the meridional gradient of SST (units: K/100 km), and (i) the meridional gradient of the net heat flux at the sea surface (units: $W \cdot m^{-2} \cdot 1000 \text{ km}^{-1}$) where the negative values indicate the downward fluxes. The terms in tendency diagnostic equation of meridional temperature gradient at 850 hPa (units: $K \cdot day^{-1} \cdot 1000 \text{ km}^{-1}$) are given in (j) horizontal advection, (k) vertical advection, and (l) diabatic heating. The black dots denote the area with significance of 95% confidence level by student-t test. The green boxes indicate the key response area.

term in the tendency diagnostic equation of meridional temperature gradient to determine the impact of the horizontal temperature advection. The diagnostic results show that the horizontal temperature advection is the main factor for the occurrence of the abnormal atmospheric baroclinicity over the North Atlantic in the concurrent winter of ENSO events (Figure 3j). The impact of vertical temperature advection almost counteracts that of diabatic heating (Figures 3k and 3l). The horizontal temperature advection driven by the anomalous westerly jet stream over the North Pacific results in enhanced (reduced) atmospheric baroclinicity over the key response area in the concurrent winter of El Niño (La Niña) events. The change in the atmospheric baroclinicity determines the generation location of the ECs over the North Atlantic, thereby causing disparity in the translation of the ECs from the North Atlantic into the polar regions, and ultimately inducing corresponding SLP anomalies pattern of the AO phases in the concurrent winter.

OIAN ET AL. 7 of 12

4. Summary and Discussion

This study reveals that during the three types of El Niño (La Niña) events, the Arctic region shows a significant SLP anomaly pattern associated with the AO negative (positive) phase in the concurrent winter (DJF0). However, the manifestations of the AO in the following winter (DJF1) are completely different. For individual El Niño (La Niña) events, the SLP field over the extratropics in the following winter (DJF1) is only affected by the poleward propagating atmospheric angular momentum induced by the ENSO event of the previous year (DJF0), presenting a positive (negative) AO phase. For double and opposite ENSO events, the AO in the following winter (DJF1) is also simultaneously affected by the ENSO events in the previous winter (DJF0) and following winter (DJF1). Among them, for the opposite El Niño (La Niña) events, the amplitude of the AO in the following winter (DJF1) is amplified by the ENSO event in the same winter (DJF1), showing a stronger positive (negative) AO phase. However, for the double El Niño (La Niña) events, the Arctic region shows SLP anomalies of the AO negative (positive) phase in the following winter (DJF0), which is dominated by the ENSO events in the same winter (DJF1). This indicates that the concurrent influence (DJF0) of ENSO on the AO is more significant than the one-year-lagged influence (DJF1) through the poleward propagating atmospheric angular momentum.

The discrepancy in the genesis locations of ECs over the North Atlantic is an important element for the occurrence of the different AO phases in the concurrent winter of ENSO events. During El Niño (La Niña) years, the abnormal atmospheric temperature distribution over the North Atlantic leads to the enhancement (reduction) of atmospheric baroclinicity in the key response area, resulting in the increase (decrease) of baroclinic energy conversion from the EAPE to the EKE, whereas the barotropic energy conversion from the MKE to the EKE is negligible. Meanwhile, the genesis locations of ECs over the North Atlantic are shifted southward (northward), and thus the number of ECs entering the Arctic from the North Atlantic decreases (increases). According to Qian et al. (2025), the exchange of the ECs between the polar region and the mid-latitudes can modulate the SLP fields over the Arctic through thermodynamic and dynamic processes, further inducing the occurrence of negative (positive) AO phases in the concurrent winter of ENSO events.

Further investigation demonstrates that during ENSO events, the anomalous atmospheric temperature over the North Atlantic is not dominated by the forcing of SST in the North Atlantic, although the distribution of SST anomaly is consistent with that of temperature anomaly in the North Atlantic region. The horizontal heat advection driven by the anomalous westerly jet stream over the North Pacific, determines the anomalous temperature distribution over the North Atlantic. The westerly wind south to the climatological jet axis over the North Pacific intensifies in El Niño (La Niña) winter (Quadrelli & Wallace, 2002; Shapiro et al., 2001), bringing horizontal temperature advection toward the North Atlantic. The horizontal heat advection causes the anomalous meridional temperature gradient in the key response area, whereas the effects of vertical temperature advection and diabatic heating on the meridional temperature gradient nearly offset each other. The changes in the meridional temperature gradient dominates the enhancement (weakening) of the atmospheric baroclinicity in this region.

In brief, as shown in the schematic diagram (Figure 4), the tropical warm East Pacific SST in the El Niño winter leads to the intensification of westerly wind south to the climatological jet axis over the North Pacific which further influences the downstream North Atlantic jet stream by the eastward propagating Rossby wave. The southward shifted horizontal heat advection from the North Pacific to the North Atlantic caused by the southward shifted jet stream results in the enhancement of Eady growth rate in the key response area. The enhancement of the Eady growth rate indicates the intensification of the baroclinicity. Due to the enhanced baroclinicity in the key response area, the genesis location of the ECs over the North Atlantic displaces southward resulting in the decrease of the poleward translation of the ECs. Ultimately, the anomalous SLP pattern of the AO negative phase is induced by the thermodynamic and dynamic processes associated with the ECs activities in the concurrent winter. This physical mechanism is the opposite in La Niña events.

There are still particular differences in the SLP anomalies over the Artic region (Figure 1b–1d) in the concurrent winter of distinct ENSO types. This is because, besides the influence of ENSO, the AO is also affected by the stratospheric polar vortex in the Arctic (Baldwin & Dunkerton, 2001; Baldwin et al., 2003) and the atmospheric internal variability (Thompson & Wallace, 1998) in the concurrent winter. The different downward intrusion of the stratospheric potential vorticity may be the reason for the differences in the AO during the concurrent winter among the different ENSO types (Figure S7 in Supporting Information S1). In subsequent studies, it is necessary to further explore the synergy effect of ENSO and the stratospheric polar vortex on the AO. In addition, the spatial

OIAN ET AL. 8 of 12

 $from \ https://agupubs.onlinelibrary.wiley.com/doi/10.1029/2025GL116719\ by\ NICE,\ National\ Institute$

for Health and Care Excellence, Wiley Online Library on [22/10/2025]. See

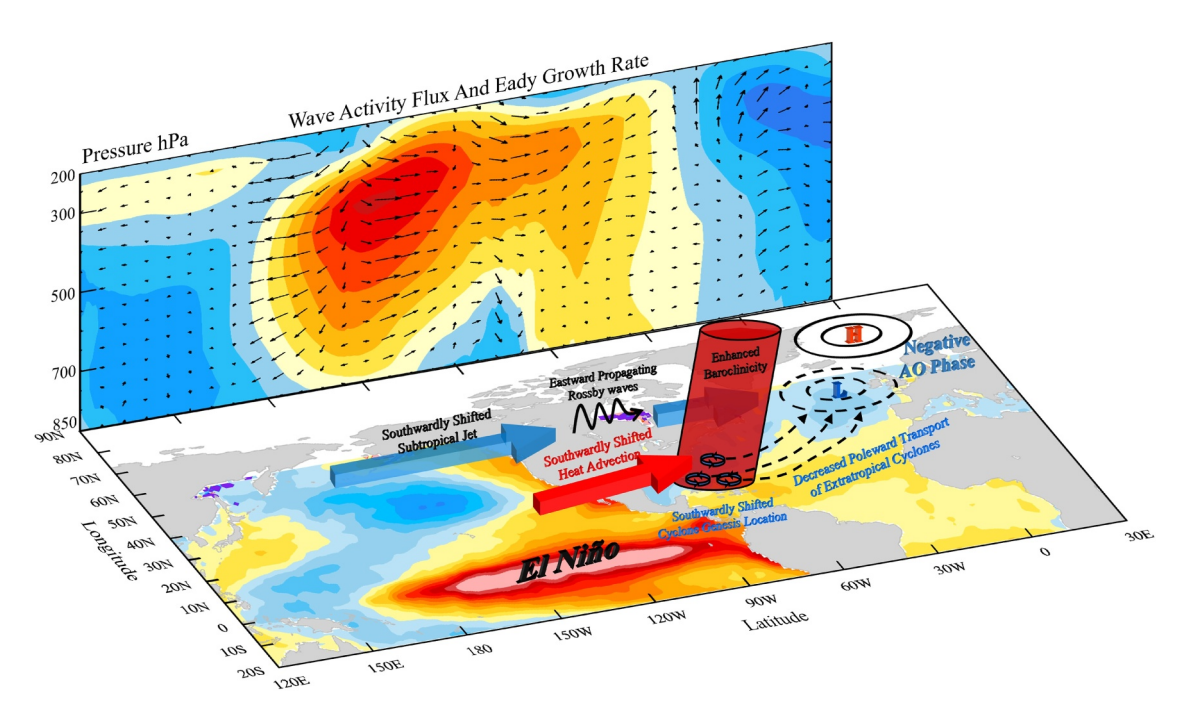


Figure 4. Schematic diagram showing how the El Niño-Southern Oscillation (ENSO) impact the Arctic Oscillation (AO) in the concurrent winter by modulating the poleward translation of the extratropical cyclones (ECs) over the North Atlantic. The horizontal figure illustrates the sea surface temperature anomaly (units: K) composite of total ENSO events (El Niño minus La Niña) in the concurrent winter. The vertical profile figure illustrates the Eady growth rate (shadings, units: 10^{-6} s^{-1}) and the wave activity fluxes (vector, units: for horizontal component $m^2 \text{ s}^{-2}$; for vertical component $10^{-2} \text{ m}^2 \text{ s}^{-2}$). The blue vectors aloft represent the subtropical westerly jet stream. The red vector aloft represents the horizontal heat advection. The black curve aloft represents the Rossby waves. The tilted cylinder represents the atmospheric baroclinicity. The cyclonic circles represent the ECs over the North Atlantic. The dashed curves represent the moving direction of the ECs. The soiled and dashed ovals represent the anomalous sea level pressure pattern of the corresponding AO phase.

diversity of ENSO (e.g., Eastern Pacific and Central Pacific types) should be also considered in the research of impact of ENSO on the AO.

Conflict of Interest

The authors declare no conflicts of interest relevant to this study.

Data Availability Statement

The ensemble mean of the 20CRv3 data set can be obtained from the NOAA Physical Sciences Laboratory (https://psl.noaa.gov/data/gridded/data.20thC_ReanV3.html), whereas the 80 members of 20CRv3 data set are able to be downloaded from the National Energy Research Scientific Computing Center (https://portal.nersc.gov/project/20C_Reanalysis/). The HadISST and the HadSLP2 data sets are provided by the Met Office Hadley Center (https://www.metoffice.gov.uk/hadobs/).

References

Allan, R., & Ansell, T. (2006). A new globally complete monthly historical gridded mean sea level pressure dataset (HadSLP2): 1850-2004 [Dataset]. *Journal of Climate*, 19(22), 5816–5842. https://doi.org/10.1175/Jcli3937.1

Ambaum, M. H. P., Hoskins, B. J., & Stephenson, D. B. (2001). Arctic oscillation or North Atlantic oscillation? *Journal of Climate*, 14(16), 3495–3507. https://doi.org/10.1175/1520-0442(2001)014<3495:Aoonao>2.0.Co;2

Anthes, R. A., Kuo, Y. H., & Gyakum, J. R. (1983). Numerical simulations of a case of explosive marine cyclogenesis. *Monthly Weather Review*, 111(6), 1174–1188. https://doi.org/10.1175/1520-0493(1983)111<1174:Nsoaco>2.0.Co;2

Arblaster, J. M., & Alexander, L. V. (2012). The impact of the El Nino-southern oscillation on maximum temperature extremes. *Geophysical Research Letters*, 39(20), L20702. https://doi.org/10.1029/2012gl053409

Ashok, K., Behera, S. K., Rao, S. A., Weng, H. Y., & Yamagata, T. (2007). El Nino Modoki and its possible teleconnection. *Journal of Geophysical Research*, 112(C11), C11007. https://doi.org/10.1029/2006jc003798

Baldwin, M. P., Cheng, X. H., & Dunkerton, T. J. (1994). Observed correlations between winter-mean tropospheric and stratospheric circulation anomalies. Geophysical Research Letters, 21(12), 1141–1144. https://doi.org/10.1029/94gl01010

OIAN ET AL. 9 of 12

Acknowledgments

Change.

(Met Office Hadley Centre) for offering guidance on the initial data analysis. Support for the Twentieth Century Reanalysis Project version 3 data set is provided by the U.S. Department of Energy, Office of Science Biological and Environmental Research (BER), by the National Oceanic and Atmospheric Administration Climate Program Office, and by the NOAA Earth System Research Laboratory Physical Sciences Laboratory. The authors sincerely thank the anonymous reviewers for their constructive comments on this paper, which have played a significant role in improving the quality of this article. This work was supported by the National Key Program for developing Basic Science (Grants 2022YFF0801702 and 2022YFE0106600), and the National Natural Science Foundation of China (Grants 42175060). The authors are thankful for the support of the Jiangsu Provincial Innovation Center for Climate

We are grate thankful to Adam A. Scaife

- Baldwin, M. P., & Dunkerton, T. J. (1999). Propagation of the Arctic oscillation from the stratosphere to the troposphere. *Journal of Geophysical Research*, 104(D24), 30937–30946. https://doi.org/10.1029/1999jd900445
- Baldwin, M. P., & Dunkerton, T. J. (2001). Stratospheric harbingers of anomalous weather regimes. Science, 294(5542), 581–584. https://doi.org/10.1126/science.1063315
- Baldwin, M. P., Stephenson, D. B., Thompson, D. W. J., Dunkerton, T. J., Charlton, A. J., & O'Neill, A. (2003). Stratospheric memory and skill of extended-range weather forecasts. *Science*, 301(5633), 636–640. https://doi.org/10.1126/science.1087143
- Barnston, A. G., & Livezey, R. E. (1987). Classification, seasonality and persistence of low-frequency atmospheric circulation patterns. *Monthly Weather Review*, 115(6), 1083–1126. https://doi.org/10.1175/1520-0493(1987)115<1083:Csapol>2.0.Co;2
- Bengtsson, L., Hagemann, S., & Hodges, K. I. (2004). Can climate trends be calculated from reanalysis data? *Journal of Geophysical Research*, 109(D11), D11111. https://doi.org/10.1029/2004jd004536
- Bjerknes, J. (1969). Atmospheric teleconnections from the equatorial Pacific. Monthly Weather Review, 97(3), 163–172. https://doi.org/10.1175/1520-0493(1969)097<0163:ATFTEP>2.3.CO:2
- Cai, M., Yang, S., den Van Dool, H. M., & Kousky, V. E. (2007). Dynamical implications of the orientation of atmospheric eddies: A local energetics perspective. *Tellus Series a-Dynamic Meteorology and Oceanography*, 59(1), 127–140. https://doi.org/10.1111/j.1600-0870.2006. 00213.x
- Cai, W. J., Ng, B., Geng, T., Jia, F., Wu, L. X., Wang, G. J., et al. (2023). Anthropogenic impacts on twentieth-century ENSO variability changes. Nature Reviews Earth & Environment, 4(6), 407–418. https://doi.org/10.1038/s43017-023-00427-8
- Cai, W. J., Santoso, A., Collins, M., Dewitte, B., Karamperidou, C., Kug, J. S., et al. (2021). Changing El Nino-southern oscillation in a warming climate. *Nature Reviews Earth & Environment*, 2(9), 628–644. https://doi.org/10.1038/s43017-021-00199-z
- Cai, W. J., Wang, G. J., Dewitte, B., Wu, L. X., Santoso, A., Takahashi, K., et al. (2018). Increased variability of eastern Pacific El Nino under greenhouse warming. Nature, 564(7735), 201–206. https://doi.org/10.1038/s41586-018-0776-9
- Capotondi, A., Wittenberg, A. T., Newman, M., Di Lorenzo, E., Yu, J. Y., Braconnot, P., et al. (2015). Understanding ENSO diversity. Bulletin of the American Meteorological Society, 96(6), 921–938. https://doi.org/10.1175/Bams-D-13-00117.1
- Chen, S. F., Chen, W., Xie, S. P., Yu, B., Wu, R. G., Wang, Z. B., et al. (2024). Strengthened impact of boreal winter North Pacific oscillation on ENSO development in warming climate. *Npi Climate and Atmospheric Science*, 7(1), 69. https://doi.org/10.1038/s41612-024-00615-3
- Choi, K. Y., Vecchi, G. A., & Wittenberg, A. T. (2013). ENSO transition, duration, and amplitude asymmetries: Role of the nonlinear wind stress
- coupling in a conceptual model. *Journal of Climate*, 26(23), 9462–9476. https://doi.org/10.1175/Jcli-D-13-00045.1

 Dai, A., Fung, I. Y., & DelGenio, A. D. (1997). Surface observed global land precipitation variations during 1900-88. *Journal of Climate*, 10(11), 2042–2042. https://doi.org/10.1175/Jcli-D-13-00045.1
- 2943–2962. https://doi.org/10.1175/1520-0442(1997)010<2943:Soglpv>2.0.Co;2
 Deser, C. (2000). On the teleconnectivity of the Arctic Oscillation. *Geophysical Research Letters*, 27(6), 779–782. https://doi.org/10.1029/
- 1999gl010945
 Eichler, T., & Higgins, W. (2006). Climatology and ENSO-Related variability of North American extratropical cyclone activity. *Journal of*
- Climate, 19(10), 2076–2093. https://doi.org/10.1175/Jcli3725.1 Feldstein, S. B., & Franzke, C. (2006). Are the North Atlantic oscillation and the northern annular mode distinguishable? *Journal of the At-*
- mospheric Sciences, 63(11), 2915–2930. https://doi.org/10.1175/Jas3798.1
 Fu, C. B., Diaz, H. F., & Fletcher, J. O. (1986). Characteristics of the response of sea-surface temperature in the Central Pacific associated with
- Fu, C. B., Diaz, H. F., & Fletcher, J. O. (1986). Characteristics of the response of sea-surface temperature in the Central Pacific associated with warm episodes of the southern oscillation. *Monthly Weather Review*, 114(9), 1716–1738. https://doi.org/10.1175/1520-0493(1986)114<1716: Cotros>2.0.Co;2
- Grise, K. M., Son, S. W., & Gyakum, J. R. (2013). Intraseasonal and interannual variability in North American storm tracks and its relationship to equatorial Pacific variability. *Monthly Weather Review*, 141(10), 3610–3625. https://doi.org/10.1175/Mwr-D-12-00322.1
- Hawkins, E., Brohan, P., Burgess, S. N., Burt, S., Compo, G. P., Gray, S. L., et al. (2023). Rescuing historical weather observations improves quantification of severe windstorm risks. *Natural Hazards and Earth System Sciences*, 23(4), 1465–1482. https://doi.org/10.5194/nhess-23-1465-2023
- Hodges, K. I. (1994). A general-method for tracking analysis and its application to meteorological data. *Monthly Weather Review*, 122(11), 2573–2586. https://doi.org/10.1175/1520-0493(1994)122<2573:Agmfta>2.0.Co;2
- Hodges, K. I. (1995). Feature tracking on the unit-sphere. *Monthly Weather Review*, 123(12), 3458–3465. https://doi.org/10.1175/1520-0493 (1995)123<3458:Ftotus>2.0.Co;2
- Hodges, K. I. (1996). Spherical nonparametric estimators applied to the UGAMP model integration for AMIP. *Monthly Weather Review*, 124(12), 2914–2932. https://doi.org/10.1175/1520-0493(1996)124<2914:Sneatt>2.0.Co;2
- Hodges, K. I. (1999). Adaptive constraints for feature tracking. *Monthly Weather Review*, 127(6), 1362–1373. https://doi.org/10.1175/1520-0493 (1999)127<1362:Acfft>2.0.Co;2
- Hoskins, B. J., & Hodges, K. I. (2002). New perspectives on the Northern hemisphere winter storm tracks. *Journal of the Atmospheric Sciences*, 59(6), 1041–1061. https://doi.org/10.1175/1520-0469(2002)059<1041:Npotnh>2.0.Co:2
- Hoskins, B. J., & Hodges, K. I. (2005). A new perspective on southern hemisphere storm tracks. *Journal of Climate*, 18(20), 4108–4129. https://doi.org/10.1175/Jcli3570.1
- Hoskins, B. J., & Karoly, D. J. (1981). The steady linear response of a spherical atmosphere to thermal and orographic forcing. *Journal of the Atmospheric Sciences*, 38(6), 1179–1196. https://doi.org/10.1175/1520-0469(1981)038<1179:Tslroa>2.0.Co;2
- Hoskins, B. J., & Valdes, P. J. (1990). On the existence of storm-tracks. *Journal of the Atmospheric Sciences*, 47(15), 1854–1864. https://doi.org/10.1175/1520-0469(1990)047<1854:Oteost>2.0.Co;2
- Hurrell, J. W. (1995). Decadal trends in the North-Atlantic oscillation Regional temperatures and precipitation. Science, 269(5224), 676–679. https://doi.org/10.1126/science.269.5224.676
- Inatsu, M., & Terakura, K. (2012). Wintertime extratropical cyclone frequency around Japan. Climate Dynamics, 38(11–12), 2307–2317. https://doi.org/10.1007/s00382-011-1152-8
- Kao, H. Y., & Yu, J. Y. (2009). Contrasting Eastern-Pacific and Central-Pacific types of ENSO. Journal of Climate, 22(3), 615–632. https://doi.org/10.1175/2008icli2309.1
- Kug, J. S., & Ham, Y. G. (2011). Are there two types of La Nina? Geophysical Research Letters, 38(16). https://doi.org/10.1029/2011gl048237
 Li, Y., & Lau, N. C. (2012). Impact of ENSO on the atmospheric variability over the North Atlantic in late winter-role of transient eddies. Journal of Climate, 25(1), 320–342. https://doi.org/10.1175/Jcli-D-11-00037.1
- Lindzen, R. S., & Farrell, B. (1980). A simple approximate result for the maximum growth-rate of Baroclinic instabilities. *Journal of the Atmospheric Sciences*, 37(7), 1648–1654. https://doi.org/10.1175/1520-0469(1980)037<1648:Asarft>2.0.Co;2

OIAN ET AL. 10 of 12

- Lu, K. C., Li, Y. R., Hu, H. B., & Wang, Z. Y. (2025). Optimized lagged multiple linear regression model for MJO prediction: Considering the surface and subsurface oceanic processes over the maritime continent. *Journal of Ocean University of China*, 24(4), 840–850. https://doi.org/10.1007/s11802-025-6082-x
- Machado, J. P., Justino, F., & Souza, C. D. (2021). Influence of El Nino-Southern oscillation on baroclinic instability and storm tracks in the Southern Hemisphere. *International Journal of Climatology*, 41(S1), E93–E109. https://doi.org/10.1002/joc.6651
- Manney, G. L., Hegglin, M. I., & Lawrence, Z. D. (2021). Seasonal and regional signatures of ENSO in upper tropospheric jet characteristics from reanalyses. *Journal of Climate*, 34(22), 9181–9200. https://doi.org/10.1175/Jcli-D-20-0947.1
- McPhaden, M. J., Zebiak, S. E., & Glantz, M. H. (2006). ENSO as an integrating concept in Earth science. Science, 314(5806), 1740–1745. https://doi.org/10.1126/science.1132588
- Neelin, J. D., Jin, F. F., & Syu, H. H. (2000). Variations in ENSO phase locking. *Journal of Climate*, 13(14), 2570–2590. https://doi.org/10.1175/1520-0442(2000)013<2570: Viepl>2.0.Co;2
- Plante, M., Son, S. W., Atallah, E., Gyakum, J., & Grise, K. (2015). Extratropical cyclone climatology across eastern Canada. *International Journal of Climatology*, 35(10), 2759–2776. https://doi.org/10.1002/joc.4170
- Qian, S. Y., Hu, H. B., Hodges, K. I., & Yang, X. Q. (2025). Do extratropical cyclones impact synoptic-scale variability of the Arctic oscillation during cold season? *Geophysical Research Letters*, 52(2), e2024GL112747. https://doi.org/10.1029/2024GL112747
- Quadrelli, R., & Wallace, J. M. (2002). Dependence of the structure of the Northern Hemisphere annular mode on the polarity of ENSO.
- Geophysical Research Letters, 29(23). https://doi.org/10.1029/2002gl015807

 Rasmusson, E. M., & Carpenter, T. H. (1982). Variations in tropical sea-surface temperature and surface wind fields associated with the southern oscillation El-Nino. Monthly Weather Review, 110(5), 354–384. https://doi.org/10.1175/1520-0493(1982)110<0354:Vitsst>2.0.Co;2
- Rayner, N. A., Parker, D. E., Horton, E. B., Folland, C. K., Alexander, L. V., Rowell, D. P., et al. (2003). Global analyses of sea surface temperature, sea ice, and night marine air temperature since the late nineteenth century [Dataset]. *Journal of Geophysical Research*, 108(D14). https://doi.org/10.1029/2002id002670
- Reboita, M. S., da Rocha, R. R., Ambrizzi, T., & Gouveia, C. D. (2015). Trend and teleconnection patterns in the climatology of extratropical cyclones over the Southern Hemisphere. *Climate Dynamics*, 45(7–8), 1929–1944. https://doi.org/10.1007/s00382-014-2447-3
- Roebber, P. J. (1984). Statistical-analysis and updated climatology of explosive cyclones. Monthly Weather Review, 112(8), 1577–1589. https://doi.org/10.1175/1520-0493(1984)112<1577:Saauco>2.0.Co;2
- Sanders, F., & Gyakum, J. R. (1980). Synoptic-dynamic climatology of the bomb. *Monthly Weather Review*, 108(10), 1589–1606. https://doi.org/10.1175/1520-0493(1980)108<1589:Sdcot>2.0.Co;2
- Scaife, A. A., Dunstone, N., Hardiman, S., Ineson, S., Li, C. F., Lu, R. Y., et al. (2024). ENSO affects the North Atlantic Oscillation 1 year later. Science, 386(6717), 82–86. https://doi.org/10.1126/science.adk4671
- Scaife, A. A., Hermanson, L., van Niekerk, A., Andrews, M., Baldwin, M. P., Belcher, S., et al. (2022). Long-range predictability of extratropical climate and the length of day. *Nature Geoscience*, 15(10), 789–793. https://doi.org/10.1038/s41561-022-01037-7
- Schemm, S., Rivière, G., Ciasto, L. M., & Li, C. (2018). Extratropical cyclogenesis changes in connection with tropospheric ENSO teleconnections to the North Atlantic: Role of stationary and transient waves. *Journal of the Atmospheric Sciences*, 75(11), 3943–3964. https://doi.
- org/10.1175/Jas-D-17-0340.1
 Shapiro, M. A., Wernli, H., Bond, N. A., & Langland, R. (2001). The influence of the 1997-99 El Nino Southern oscillation on extratropical Baroclinic life cycles over the eastern North Pacific. *Quarterly Journal of the Royal Meteorological Society*, 127(572), 331–342. https://doi.
- org/10.1002/qj.49712757205

 Slivinski, L. C., Compo, G. P., Whitaker, J. S., Sardeshmukh, P. D., Giese, B. S., McColl, C., et al. (2019). Towards a more reliable historical reanalysis: Improvements for version 3 of the twentieth century reanalysis system [Dataset]. *Quarterly Journal of the Royal Meteorological Society*, 145(724), 2876–2908. https://doi.org/10.1002/qj.3598
- Takaya, K., & Nakamura, H. (2001). A formulation of a phase-independent wave-activity flux for stationary and migratory quasigeostrophic eddies on a zonally varying basic flow. *Journal of the Atmospheric Sciences*, 58(6), 608–627. https://doi.org/10.1175/1520-0469(2001) 058<0608:Afoapi>2.0.Co;2
- Thompson, D. W. J., & Wallace, J. M. (1998). The Arctic oscillation signature in the wintertime geopotential height and temperature fields. Geophysical Research Letters, 25(9), 1297–1300. https://doi.org/10.1029/98g100950
- Timmermann, A., An, S. I., Kug, J. S., Jin, F. F., Cai, W. J., Capotondi, A., et al. (2018). El Nino-southern oscillation complexity. *Nature*, 559(7715), 535–545. https://doi.org/10.1038/s41586-018-0252-6
- Tokinaga, H., Richter, I., & Kosaka, Y. (2019). ENSO influence on the Atlantic Nino, revisited: Multi-Year versus individual-year ENSO events. Journal of Climate, 32(14), 4585–4600. https://doi.org/10.1175/Jcli-D-18-0683.1
- Toniazzo, T., & Scaife, A. A. (2006). The influence of ENSO on winter North Atlantic climate. Geophysical Research Letters, 33(24). https://doi.org/10.1029/2006g1027881
- Trenberth, K. E. (1997). The definition of El niño. Bulletin of the American Meteorological Society, 78(12), 2771–2778. https://doi.org/10.1175/1520-0477(1997)078<2771:TDOENO>2.0.CO;2
- Trenberth, K. E., Branstator, G. W., Karoly, D., Kumar, A., Lau, N. C., & Ropelewski, C. (1998). Progress during TOGA in understanding and modeling global teleconnections associated with tropical sea surface temperatures. *Journal of Geophysical Research*, 103(C7), 14291–14324. https://doi.org/10.1029/97jc01444
- Wallace, J. M. (2000). North Atlantic oscillation/annular mode: Two paradigms One phenomenon. *Quarterly Journal of the Royal Meteorological Society*, 126(564), 791–805. https://doi.org/10.1256/smsqj.56401
- Wallace, J. M., & Thompson, D. W. J. (2002). The Pacific center of action of the Northern hemisphere annular mode: Real or artifact? *Journal of Climate*, 15(14), 1987–1991. https://doi.org/10.1175/1520-0442(2002)015<1987:Tpcoao>2.0.Co;2
- Wang, H. S., & Mullens, E. (2024). Role of individual and compound Pacific natural variability in extratropical cyclone activity over North America. International Journal of Climatology, 44(2), 647–667. https://doi.org/10.1002/joc.8349
- Wang, T., Gou, X. H., Wang, X. J., Liu, H. W., & Xie, F. (2024). Equatorward shift of ENSO-related subtropical jet anomalies in recent decades. Atmospheric Research, 297, 107109. https://doi.org/10.1016/j.atmosres.2023.107109
- Wang, X. L. L., Feng, Y., Chan, R., & Isaac, V. (2016). Inter-comparison of extra-tropical cyclone activity in nine reanalysis datasets. Atmospheric Research, 181, 133–153. https://doi.org/10.1016/j.atmosres.2016.06.010
- Wang, X. L. L., Feng, Y., Compo, G. P., Swail, V. R., Zwiers, F. W., Allan, R. J., & Sardeshmukh, P. D. (2013). Trends and low frequency variability of extra-tropical cyclone activity in the ensemble of twentieth century reanalysis. *Climate Dynamics*, 40(11–12), 2775–2800. https://doi.org/10.1007/s00382-012-1450-9
- Yanai, M., Esbensen, S., & Chu, J. H. (1973). Determination of bulk properties of tropical cloud clusters from large-scale heat and moisture budgets. *Journal of the Atmospheric Sciences*, 30(4), 611–627. https://doi.org/10.1175/1520-0469(1973)030<0611:Dobpot>2.0.Co;2

QIAN ET AL.



Geophysical Research Letters

10.1029/2025GL116719

Yeh, S. W., Cai, W. J., Min, S. K., McPhaden, M. J., Dommenget, D., Dewitte, B., et al. (2018). ENSO atmospheric teleconnections and their response to greenhouse gas forcing. *Reviews of Geophysics*, 56(1), 185–206. https://doi.org/10.1002/2017rg000568

Yoshiike, S., & Kawamura, R. (2009). Influence of wintertime large-scale circulation on the explosively developing cyclones over the western North Pacific and their downstream effects. *Journal of Geophysical Research*, 114(D13). https://doi.org/10.1029/2009jd011820

Yu, P., Qian, S., Hu, H., He, S., Xiong, Y., Fu, T., & Wang, Y. (2025). Synergistic influences from high, middle, and low latitudes on the extreme precipitation events in the Beijing-Tianjin-Hebei region during the summer of 2023. *Journal of Ocean University of China*, 24(5), 1157–1168. https://doi.org/10.1007/s11802-025-6107-5

QIAN ET AL. 12 of 12